Open Veterinary Journal, (2023), Vol. 13(5): 645–653
ISSN: 2226-4485 (Print)
ISSN: 2218-6050 (Online)
Original Research
DOI: *10.5455/OVJ.2023.v13.i5.18*

Submitted: 02/02/2023 Accepted: 26/04/2023 Published: 21/05/2023

Ex-vivo biomechanical analysis of an original repair of canine calcaneal tendon rupture using a synthetic implant as mechanical support fixed by sutures in the proximal tendinous part and by an interference screw in the bone distal part

Philippe Buttin[1†], Bastien Goin[2,3,4*†], Antonin Jean Johan Crumière[4], Eric Viguier[2], Michel Massenzio[3], Yoann Lafon[3] and Thibaut Cachon[2]

[1]*Itinerant Surgeon, Villaz, France*
[2]*Université de Lyon, VetAgro Sup, Interactions Cellules Environnement (ICE), Marcy l'Etoile, France*
[3]*Univ Lyon, Univ Gustave Eiffel, Univ Claude Bernard Lyon 1, Lyon, France*
[4]*Novetech Surgery, Monaco, Monaco*
[†]*These authors contributed equally to this work*

Abstract

Background: Rupture of the common calcaneal tendon is the second most frequent tendon rupture in dogs and may lead to severe lameness and pain. Surgical repair consists of re-apposition of the damaged tendon ends using sutures, but this type of repair is not always possible especially if the tendon has retracted. Tendon augmentation with an ultra-high molecular weight polyethylene (UHMWPE) implant is a recent solution to support the sutures and allow the repair of the canine calcaneal tendon. However, its biomechanical fixation strength remains untested for this pathology.

Aim: To evaluate the biomechanical fixation strength of a UHMWPE implant for the repair of the canine calcaneal tendon.

Methods: *Ex-vivo* biomechanical study was carried out on eight cadaveric hindlimbs from four adult dogs. Hindlimbs were tested under two independent modalities: proximal tendinous fixation (PTF) and distal calcaneus fixation (DCF), using a testing machine. PTF was achieved by eight simple interrupted polypropylene sutures performed through the UHMWPE implant. The latter was sandwiched inside the gastrocnemius tendon, which had previously been incised over about 5 cm longitudinally, and through the tendon of the superficial digital flexor. DCF was performed using an interference screw, which locked the UHMWPE implant into a calcaneus tunnel drilled perpendicularly.

Results: Yield, failure load, and linear stiffness (mean ± SD) for the DCF modality were 920 ± 139 N, 1,007 ± 146 N, and 92 ± 15.21, respectively, which were greater than for the PTF modality (663 ± 92 N, 685 ± 84 N and 25.71 ± 5.74, respectively, $p < 0.05$). Failure modes were different between fixation modalities: for PTF it was suture breakage (n = 7/8), while for DCF it was implant damage and slippage (n = 8/8).

Conclusion: The biomechanical fixation strength of the UHMWPE implant was greater for DCF than that of PTF, and should be suitable for calcaneal tendon repair in dogs. The clinical prediction of rupture of this calcaneal tendon repair will occur at the level of the PTF.

Keywords: Biomechanical analysis, Dog, *ex-vivo*, Tendon repair, UHMWPE implant.

Introduction

Rupture of the common calcaneal tendon is the second most frequent tendon rupture in dogs after that of the proximal biceps tendon, which may lead to severe lameness and pain depending on severity and duration (Kása *et al*., 1994). The study published by Corr *et al*. (2010) reported that ruptures of the common calcaneal tendon in dogs are often acute at the level of the enthesis and affect all heads of the tendons (gastrocnemius, superficial flexor tendon, combined tendons of the gracilis, semitendinosus, and biceps femoris). Surgical repair consists of re-apposition of the damaged tendon ends, using various suture patterns such as the Kessler suture (Kessler, 1973), a modified Kessler knotless barbed technique (Frame *et al*., 2019), the three-loop pulley, the modified three-loop pulley and the locking loop (Moores *et al*., 2004a, 2004b). More recently, studies have shown that the addition of epitendinous sutures significantly increases the strength of mid-body tendon repairs in dogs (Duffy *et al*., 2019; Cocca *et al*., 2020; Duffy *et al*., 2020a). However, it is not always possible to suture the tendon ends, especially if the

***Corresponding Author:** Bastien Goin. Université de Lyon, VetAgro Sup, Interactions Cellules Environnement (ICE), Marcy l'Etoile, France. Email: *bastien.goin@vetagro-sup.fr*

rupture area is at the level of the calcaneal enthesis, unless one drill through the calcaneus and passes the suture inside one or two bone tunnels (Gall *et al*., 2009; Wilson *et al*., 2014; Dunlap *et al*., 2016). This difficulty may arise when the rupture of the calcaneal tendon is chronic and the proximal torn tendon ends have retracted (Buttin *et al*., 2020a). In such cases, an augmentation of the tendon is required to support the sutures (Baltzer and Rist, 2009; Gall *et al*., 2009; Ambrosius *et al*., 2015; Morton *et al*., 2015a, 2015b; Zellner *et al*., 2018; Duffy *et al*., 2020b). It can be biologic, using an autologous graft of either the semitendinosus muscle (Baltzer and Rist, 2009) or the flexor digitorum lateralis muscle (Katayama, 2016; Duffy *et al*., 2020b); metallic, using tendon plating as an augmentation technique (Zellner *et al*., 2018); or even synthetic, using a degradable porous polyurethane mesh graft (Ambrosius *et al*., 2015), a non-degradable polypropylene mesh graft (Gall *et al*., 2009), a polyethylene terephthalate braided implant (Morton *et al*., 2015a, 2015b), or an ultra-high molecular weight polyethylene (UHMWPE) braided implant (Buttin *et al*., 2020a, 2020b). The success of these techniques lies in the mechanical strength of the distal fixation used at the level of the calcaneus, such as bone tunnels (Gall *et al*., 2009), anchors (Schulz *et al*., 2019), or interference screws (Morton *et al*., 2015a, 2015b; Buttin *et al*., 2020a, 2020b). It also depends on the type of suture used to fix the proximal tendon end, such as loop sutures (Schulz *et al*., 2019), eight evenly spaced simple interrupted sutures (Morton *et al*., 2015a, 2015b; Buttin *et al*., 2020b), or overlock sutures (Goin *et al*., 2020). In canine calcaneal tendon repair, the association of these mechanical synthetic supports with proximal tendinous fixation (PTF) performed by sutures and distal calcaneus fixation (DCF) provides increased mechanical strength compared to conventional tendon suture techniques used alone. This association has shown encouraging biomechanical (Gall *et al*., 2009; Morton *et al*., 2015b; Buttin *et al*., 2020b) and clinical results (Morton *et al*., 2015a; Schulz *et al*., 2019; Buttin *et al*., 2020a). The primary objective of these techniques using synthetic mechanical support for the repair of the calcaneal tendon in dogs is to allow early postoperative weight-bearing of the affected hindlimb without resorting to transarticular immobilization, as is still the case in clinical routines with an external skeletal fixator (Nielsen and Pluhar, 2006; Zellner *et al*., 2018) or calcaneotibial screws (Moores *et al*., 2004a; Corr *et al*., 2010). The latter are associated with major complication rates of 31.3% (Nielsen and Pluhar, 2006) and 8% (Corr *et al*., 2010), respectively. Other immobilization techniques are less rigid, such as casts or splints (Nielsen and Pluhar, 2006; Baltzer and Rist, 2009; Morton *et al*., 2015a; Katayama, 2016; Frame *et al*., 2019; Schulz *et al*., 2019; Buttin *et al*., 2020a), but they still report a significant 20% complication rate when used for distal limb orthopedic conditions (Meeson *et al*., 2011). The main objective of tendon augmentation techniques using a synthetic mechanical support is to allow repair of the canine calcaneal tendon while providing a mechanical support that is strong enough to overcome any type of hindlimb immobilization during the postoperative period.

The objective of this *ex-vivo* study was to evaluate the biomechanical fixation strength of an UHMWPE implant for the repair of the canine calcaneal tendon. We hypothesized that (i) the biomechanical fixation strength of the UHMWPE implant is suitable for calcaneal tendon repair in dogs, and that (ii) PTF performed by sutures will be the weakest area compared to DCF by interference screw.

Materials and Methods

Cadaveric preparation

Anatomical parts were obtained from four large breed adult dogs weighing 35–45 kg and that had been euthanatized for reasons unrelated to the present study. Following consent, cadaveric specimens were donated by the society for the protection of animals. Owing to the provenance of the canine cadavers, the medical history of the dogs was unknown. No sign of musculoskeletal disease, trauma, defect in conformation, or area that might suggest a previous scarred trauma was reported on palpation of the hindlimbs. This was confirmed later during dissection. The canine cadaver specimens were frozen for 48 hours at −18°C less than 6 hours after euthanasia and left to thaw in a fridge at 5°C for 48 hours prior to the collection of anatomic parts. Freezing at −18°C does not alter the mechanical performance of tendons (Hirpara *et al*., 2008). Eight paired hindlimbs were harvested from the four canine cadavers on the day of the study. All soft tissues, except the gastrocnemius, superficial digital flexor (SDF) muscles, and tendons, were removed from the hindlimb. The femur was disarticulated from the tibia, fibula, and patella, and the calcaneus was disarticulated from the tibia, fibula, talus, and fourth metacarpal bone. The gastrocnemius tendon was released from the tuber calcanei enthesis, then the tendon of the SDF was transversely transected at the same level as the gastrocnemius tendon enthesis. The femur and the calcaneus were also dissected. Four wood screws were implanted in the cranial part of the calcaneus to allow a better grip in the inclusion environment, and the femur was sectioned in the diaphysis area to facilitate the inclusion with resin (polyol and isocyanate, Axson Technologies, France) onto metal supports (3 × 3 × 7 cm). 8-mm drilling was carried out in a lateromedial direction through each femoral metal support 1.5 cm from each distal edge.

Implant Design

The synthetic implant (Novaten 8000, Novetech Surgery, Monaco) is manufactured from a specific braiding of UHMWPE medical-grade multi-filaments already used for orthopedic implants in several medical applications, such as anterior cruciate implants (Purchase *et al*., 2007). Once braided, the

synthetic ligament is sterilized with ethylene oxide and has greater mechanical strength than physiological tendons (8,000 N of failure strength reported by the manufacturer), with an elastic deformation estimated at 4% under 1,000 N load. It comprises two components: a flat implanted section, which is 6-mm wide and 14-cm long, designed to be sutured from the musculotendinous junction through the split tendon (Fig. 1A) and fastened to the bone at its distal end with a titanium cannulated interference screw (Fig. 1B); a puller wire allowing the insertion of the implant into the bone tunnels (Fig. 1C).

Implantation of the UHMWPE implant

For each anatomic sample, two UHMWPE implants (Novaten 8000, Novetech Surgery, Monaco) were required for testing proximal and distal surgical fixations independently. For the proximal fixation in the tendinous part, the gastrocnemius tendon was longitudinally incised over half of its diameter, from the incision at the level of the enthesis to the musculotendinous junction, over a length of 5 cm measured and controlled using a graduated ruler placed under the gastrocnemius tendon. The first UHMWPE implant was placed proximally along the whole length of the half-split tendon, then sandwiched inside the tendon incision. The tendon of the SDF was placed against the split gastrocnemius tendon to allow the sutures to pass mediolaterally through these four components: SDF tendon, the medial part of the half-split gastrocnemius tendon, UHMWPE implant, the lateral part of the half-split gastrocnemius tendon. The fixation of this four-component system was performed by eight simple interrupted sutures of 3.5 metric polypropylene (Prolene, Ethicon, Inc., Somerville, NJ). Each suture was performed using eight throws, locked with a surgeon's knot, and the suture thread was cut 3 mm from the knot. Sutures were spaced 5 mm apart and each was about 4-cm long, starting from the myotendinous junction towards the enthesis of the gastrocnemius tendon through the four-component system (Fig. 2A).

For the distal fixation in the calcaneus part, a 3.6-mm oblique bone tunnel was drilled from the tuber calcanei enthesis of the gastrocnemius tendon to the plantar surface of the calcaneus, using a cannulated drill bit on a 2-mm Kirschner wire. A second 3.6-mm perpendicular bone tunnel was drilled a few millimeters distally to the plantar exit of the first one, from the lateral to the medial side. The entry point of this second calcaneus tunnel was defined to preserve dorsal and plantar bone margins at least equivalent to the screw diameter (4.5 mm) to avoid the risk of fracture. The second calcaneus tunnel was pre-formed from the lateral surface towards the medial aspect of the calcaneus with a 4.5 × 15 or 20-mm interference screw. The second UHMWPE implant was inserted inside the first tunnel, from the tuber calcanei to the plantar surface of the calcaneus, then in the second tunnel, from the lateral surface to the medial aspect of the calcaneus via the puller wire by sliding through grommets. A 1-mm smooth pin was used as a guide to insert the 4.5 × 15 or 20-mm interference screw (chosen according to depth of the second tunnel), from the lateral surface towards the medial aspect of the calcaneus. The screw was inserted with a ratchet screwdriver following the axis of the pin to avoid the risk of fracturing the trans-cortex (Fig. 2B). Each suture and UHMWPE implant package was sterile, used before the manufacturer's expiration date, and opened immediately before use. All surgical implantations of anatomic samples were performed by the same veterinary surgeon (PB).

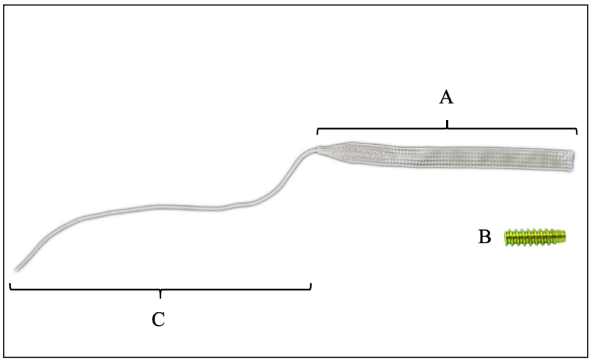

Fig. 1. UHMWPE Implant (Novaten 8000, Novetech Surgery, Monaco). The implant is made of two parts: (A) the implanted section, which is to be sutured at its proximal end to the musculotendinous junction and, (B) fastened at its distal end to the bone with a titanium canulated interference screw; (C) a puller wire for inserting the implant into the bone tunnels.

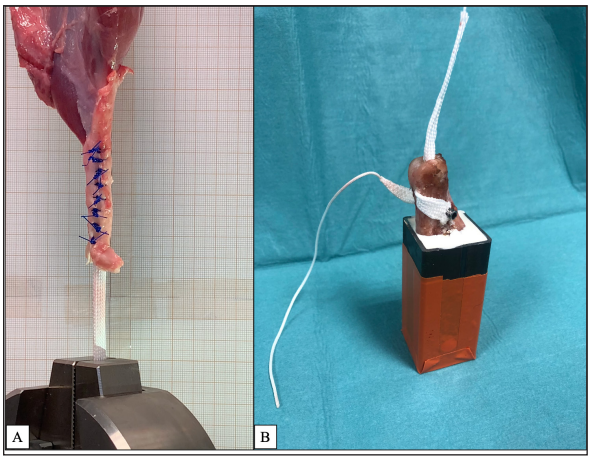

Fig. 2. (A) PTF performed through UHMWPE implant, gastrocnemius and SDF tendons, secured by eight simple interrupted sutures of 3.5 metric polypropylene, spaced 5 mm apart, about 4-cm long; (B) DCF performed using a 4.5 × 15 or 20-mm titanium canulated interference screw, which locks the UHMWPE implant in a calcaneus tunnel drilled perpendicularly.

Biomechanical testing

One anatomic sample group (hindlimb n = 8) was defined in order to evaluate the mechanical strength of two types of UHMWPE implant fixations: the PTF performed by eight simple interrupted sutures, and the DCF performed by interference screw. Each fixation modality was tested independently but following the same testing procedure. Sixteen independent static tensile tests were performed using a traction system (AGS-X Shimadzu, Japan). The testing of the PTF of the anatomical samples was ensured by a caliper connected directly to the 5KN force cell located in the traverse stroke of the mechanical testing machine, allowing the placement of an 8-mm pin through the drilling carried out previously in each metal support. This proximal pivot system, therefore, allowed perfect alignment of the forces in line with the lower mechanical grip, which mechanically held the distal part of the UHMWPE implant (Fig. 3A). The testing of the DCF by interference screw was carried out with a custom assembly (EV), allowing the simple placement of the anatomical samples in line with the mechanical traction axis of the testing machine (Fig. 3B). The samples were then tested when they had reached the ambient temperature of the biomechanics laboratory (18°C). Each tensile test started with a pre-test of 20 mm/minute traction until the load reached 30 N, straightening the system (Morton *et al*., 2015b). The tensile test consisted in 25 mm/minute traction until failure and the sampling rate for data acquisition was set at 100 Hz. A total of 16 experimental set-ups were evaluated: 8 testing the mechanical failure strength of the PTF by sutures (S1R&L, S2R&L, S3R&L, and S4R&L) (Fig. 3A) and 8 testing the mechanical failure strength of the DCF by interference screw (C1R&L, C2R&L, C3R&L, C4R&L) (Fig. 3B). Tests were named as follows: S or C for "Suture" or "Calcaneus," then the test number from 1 to 8, and finally R or L for "Right" or "Left" laterality of the hindlimb from which the anatomical sample was harvested.

Data acquisition and processing

When performing tests, data acquisition was performed with the TrapeziumX software (Shimadzu, Japan). Yield, peak, and failure forces were considered for each mechanical test of proximal and distal fixations. Yield force was defined as the force at which the first deviation from linearity occurred in the load displacement curve. Peak force was defined as the first value of the force cell recording a drop in forces compared to the previous acquired value. Failure force was defined as the maximum force measured during each test: suture breakage for PTF and sliding of the UHMWPE implant inside the bone tunnel at bone/UHMWPE implant/interference screw interface for DCF. Failure mode was recorded by video acquisition during each test (iPhone XS; Apple, Cupertino, California) (Fig. 3A). Microsoft Excel (Microsoft Excel; Microsoft, Redmond, Washington) and Matlab (R2017b; MathWorks, Natick Massachusetts) software were used to process the data.

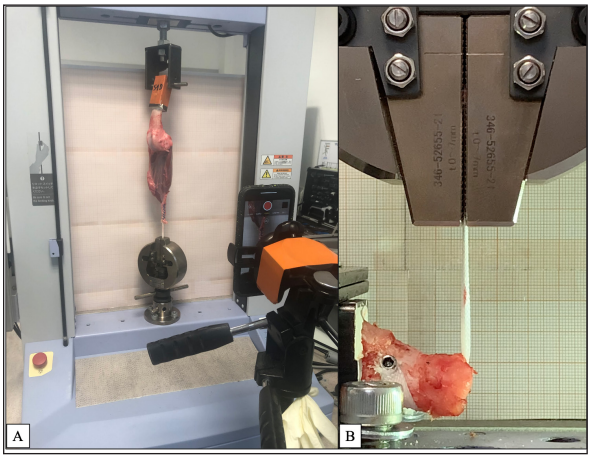

Fig. 3. (A) Biomechanical setup to evaluate mechanical strength of PTF; (B) DCF.

Statistical analysis

No *a priori* power analysis was performed during the study. *A posteriori* verification of the normality of our datasets was carried out with a Lilliefors test, although the normal distribution of the data could not be confirmed statically by the software (Matlab R2017b; MathWorks, Natick Massachusetts). Differences in stiffness, yield, peak, and failure load of both distal and proximal fixations were compared using the Wilcoxon rank-sum test (Matlab R2017b; MathWorks, Natick Massachusetts). A p-value of <0.05 was considered significant.

Results

An example of load–displacement curve was generated for S1R and C1R with a graphic display of the mechanical reference values chosen (Fig. 4).

Failure mode of PTF by sutures

After frame-by-frame video analysis, we observed that the most common failure mode of PTF was the breakage of all sutures occurring concomitantly (n = 5/8) (Table 1, Fig. 5A). The second failure mode was the most distal suture at the level of gastrocnemius tendon enthesis breaking first, followed immediately by all seven other sutures (n = 2/8). The last failure mode was the progressive delamination of the gastrocnemius and SDF musculotendinous junction (n = 1/8).

Failure mode of DCF by interference screw

After frame-by-frame video analysis, a progressive sliding of the UHMWPE implant through the two bone tunnels at the bone/implant/interference screw interface was observed for the DCF (Table 2). This slippage caused progressive damage to the UHMWPE implant in contact with the interference screw in the second calcaneus tunnel, without ever breaking it (Fig. 5B). No fracture or bone crack was observed by the veterinary surgeon (PB) after the implantation of the calcaneus interference screw inside the second tunnel. This macroscopic observation was confirmed by post-mechanical test radiographs (Fig. 6A and B).

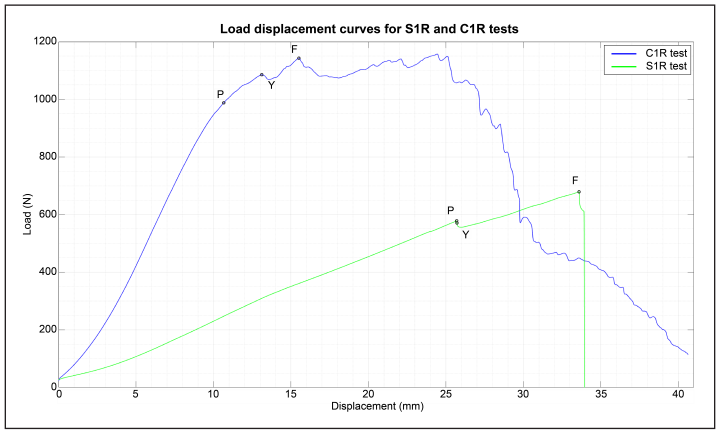

Fig. 4. Example of load displacement curves for PTF and DCF, respectively termed S1R and C1R biomechanical tests. Points Y, P and F show the yield, peak and failure load, respectively, for evaluating mechanical strength of the two fixation modalities.

Table 1. Results, mean, and standard deviation (SD) for yield, peak and failure loads, linear stiffness, and failure mode of eight static tensile tests until failure, performed on PTF by eight simple interrupted sutures of 3.5 metric polypropylene.

PTF by sutures					
Test name	**Linear stiffness (N/mm)**	**Yield load (N)**	**Peak load (N)**	**Failure load (N)**	**Failure mode**
S1R	22.42	571	578	679	DSB + [SSB]
S1L	16.58	736	746	746	[SSB]
S2R	28.65	803	809	809	[SSB]
S2L	18.89	526	535	535	PD G + SDF
S3R	28.47	650	659	659	[SSB]
S3L	33.1	718	730	730	[SSB]
S4R	28.74	687	701	701	DSB + [SSB]
S4L	28.86	611	621	621	[SSB]
Mean	25.71	663	672	685	-
SD	5.74	92	92	84	-

Acronyms: DSB + [SSB], distal suture breakage + set of suture breakage; [SSB], set of suture breakage; PD G + SDF, progressive delamination of gastrocnemius and superficial digital flexor musculotendinous junction.

Mechanical strength comparison of proximal and distal fixations

Yield, peak, and failure loads and linear stiffness for the DCF modality were statistically greater than for the PTF modality ($p < 0.05$) (Table 3).

Discussion

In agreement with our hypothesis and objective, the biomechanical strength evaluation of the PTF and DCF showed high tensile yield, peak, and failure loads. Despite differences in experimental protocols, our results are in the same range of values measured for the proximal and distal parts of both physiological SDF tendon and physiological gastrocnemius tendon, while being generally lower than these physiological mean failure loads (Jopp and Reese, 2009). The values we obtained are also superior to the estimated tensile strength of 399 N exerted on the Achilles mechanism during locomotion for a 30-kg trotting dog (Moores *et al*., 2004b), and are in the same range or even superior to those of already published tendon repair techniques (Moores *et al*., 2004a, 2004b; Gall *et al*., 2009; Wilson *et al*., 2014; Morton *et al*., 2015b; Dunlap *et al*., 2016; Duffy *et al*., 2019; Cocca *et al*., 2020; Duffy *et al*., 2020a, 2020b). In the PTF modality, high strength could be explained by the sandwiching the UHMWPE implant inside the split gastrocnemius tendon. This choice was made to provide ideal centrality of the UHMWPE implant and a better distribution of mechanical strength through the gastrocnemius tendon. Clinically, the longitudinal incision of the gastrocnemius tendon may help postoperative neovascularization at the UHMWPE implant/gastrocnemius tendon interface, thus allowing the early initiation of the tendon healing

process by fibrosis (Buttin *et al*., 2020a). The bulging of the SDF tendon through the split gastrocnemius tendon containing the UHMWPE implant in its center as initially defined in the surgical technique (Buttin *et al*., 2020a) also increases the mechanical strength of the PTF.

The choice of polypropylene rather than polydioxanone sutures (Morton *et al*., 2015a, 2015b) was made according to recently published state-of-the-art studies on tendon repair techniques (Duffy *et al*., 2019; Cocca *et al*., 2020; Duffy *et al*., 2020a, 2020b). Sutures of the PTF were performed with particular care. Indeed, once the first proximal suture close to the myotendinous junction was carried out, manual tensioning of the gastrocnemius and SDF tendon was applied with the UHMWPE implant in the direction of the gastrocnemius tendon enthesis to perform the other seven simple interrupted sutures. Failure of the PTF occurred in five out of the eight mechanical tests performed. It was a simultaneous rupture of the eight sutures, which indicates that the PTF behaves as one unified system (UHMWPE implant + eight simple interrupted sutures). This provides a homogeneous distribution of mechanical strength and therefore better failure strength.

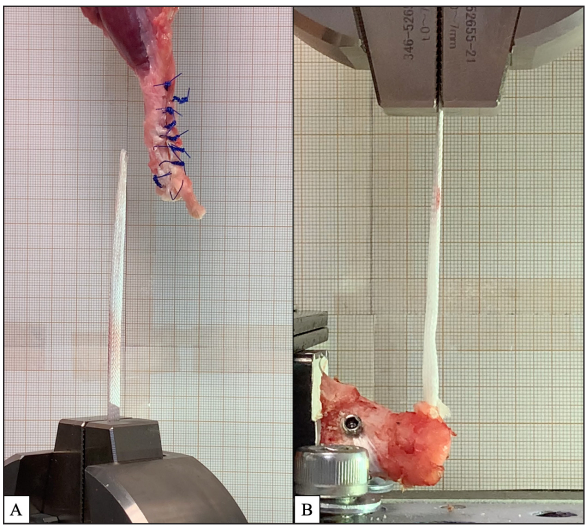

Fig. 5. Example of failure mode for (A) PTF: suture breakage (n = 7/8); (B) DCF: damage and slippage of UHMWPE implant through two bone tunnels at bone/implant/interference screw interface (n = 8/8).

The high strength observed in the DCF modality could be explained by the utilization of a titanium interference screw allowing an immediate and strong mechanical fixation of the UHMWPE implant inside the bone tunnel (Blanc *et al*., 2019; Goin *et al*., 2019). The anatomical location of the bone tunnel influences the mechanical strength of the fixation. For example, a synthetic implant secured with an interference screw in a tunnel drilled in an epiphyseal area (Blanc *et al*., 2019) will have lower pull-out strength than if fixed in a bone with higher density, such as the calcaneus (Morton *et al*., 2015b). The drilling axis of the bone tunnel also influences the pull-out strength of the interference screw fixation (Zhang *et al*., 2007; Aoki *et al*., 2019). The choice of drilling a second perpendicular tunnel in the calcaneus as a distal fixation point was made for two reasons: first, in order to increase the mechanical strength (Zhang *et al*., 2007; Aoki *et al*., 2019) of the DCF, thus allowing the formation of a 90° angle with the axis of application of in-situ mechanical forces, through the calcaneal tendon; second, because the perpendicular tunnel allows easier tensioning of the augmented canine calcaneal tendon with the UHMWPE implant before its reinsertion into the calcaneus by the interference screw (Buttin *et al*., 2020a). The DCF failed in only one way, i.e., damage and slippage of the UHMWPE implant through the two bone tunnels at the bone/implant/interference screw

Table 2. Results, mean, and standard deviation (SD) for yield, peak and failure load and failure mode of eight static tensile tests until failure, performed on DCF by 4.5 × 15 or 20-mm interference screw.

DCF by interference screw				
Test name	**Linear stiffness (N/mm)**	**Yield load (N)**	**Peak load (N)**	**Failure load (N)**
C1R	105.35	988	1,086	1,143
C1L	79.79	754	774	895
C2R	105.19	1,154	1,169	1,240
C2L	89.26	918	954	1,051
C3R	108.33	992	1,002	1,002
C3L	102.05	991	1,024	1,056
C4R	76.42	762	805	805
C4L	69.64	804	869	869
Mean	92	920	960	1,007
SD	15.21	139	138	146

Failure mode: implant damage and slippage (8/8)

interface without ever breaking. This phenomenon had already been observed in two previous biomechanical studies in which this UHMWPE implant had been used for ligament reconstruction (Blanc *et al*., 2019; Goin *et al*., 2019).

There are some variations between our technique and that of Morton *et al*. (2015b), who tested a similar procedure for gastrocnemius tendon repair. The synthetic implant tested was not the same, as one was made of polyethylene terephthalate mono-filaments (Morton *et al*., 2015b) and the other was made of UHMWPE mono-filaments, both braided but not with the same braiding technique. For the PTF, the repair technique of Morton *et al*., (2015b) did not involve a longitudinal incision of the gastrocnemius tendon in order to insert the synthetic implant, nor did it include the association of the SDF tendon during suturing or the use of sutures through and along the gastrocnemius and SDF tendon from the myotendinous junction to the distal part of the tendons. Regarding the DCF, Morton *et al*. (2015b) created a single blind-ending calcaneus tunnel while we drilled two, one of which was perpendicular. Morton *et al*. (2015b) chose to test the DCF by placing the anatomical axis of the calcaneus along the tensile axis of the mechanical testing machine. In our study, we made the choice of placing the anatomical axis of the calcaneus at a 90° angle from the mechanical axis of the traction machine. To us, this angle seemed more representative of a physiological condition of calcaneal tendon rupture in dogs. All these variations likely influenced the mechanical strength of our two fixation modalities. The type of suture used by Morton *et al*. (2015) to perform the PTF was also different (polydioxanone *vs.* polypropylene in our study). However, these two types of sutures have the same biomechanical strength when they are used as tendon sutures (O'Broin *et al*., 1995).

Our study has some limitations. First, there is the non-normal distribution of our data sets, as well as the low number of biomechanical tests carried out. Second, we tested the PTF independently of the DCF without having tested the entire canine calcaneal tendon repair

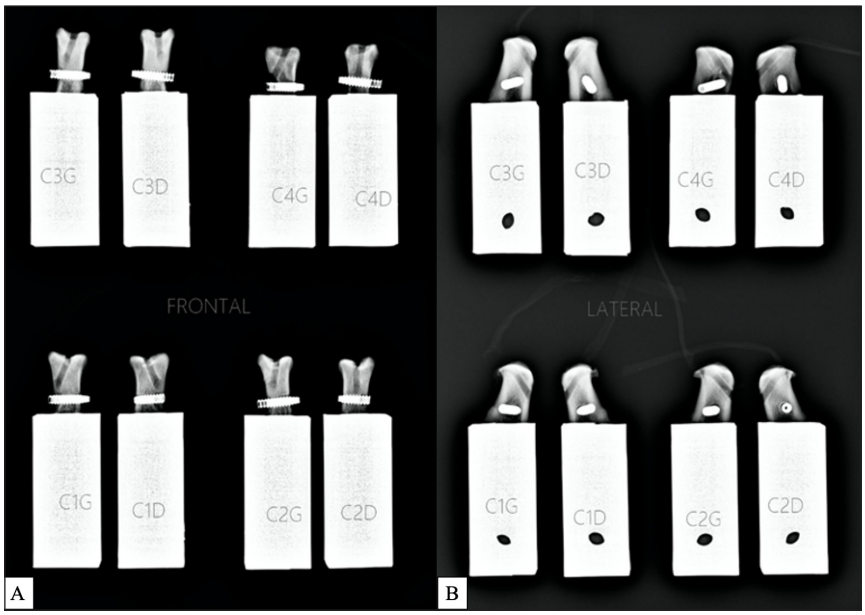

Fig. 6. Post-mechanical test radiographs of the eight DCFs: (A) frontal and (B) lateral.

Table 3. Yield, peak, and failure loads and linear stiffness for proximal and distal UHMWPE implant fixations.

Modality	Linear stiffness (N/mm)	Yield load (N)	Peak load (N)	Failure load (N)
PTF	25.71 ± 5.74*	663 ± 92*	672 ± 92*	685 ± 84*
DCF	92 ± 15.21**	920 ± 139**	960 ± 138**	1007 ± 146**

Note: Values are mean ± SD. Acronyms: PSF, proximal tendinous fixation; DCF, distal calcaneus fixation. *$p < 0.05$ difference in yield, peak, and failure loads and linear stiffness between experimental modalities. **$p < 0.05$ difference in yield, peak, and failure loads and linear stiffness between experimental modalities.

technique nor a physiological canine calcaneal tendon. This choice was driven by the limited number of anatomical parts available, and the aim of providing reliable biomechanical information from the two types of fixations since testing the entire canine calcaneal tendon repair technique would have provided only information about the weakest fixation. Third, we would have achieved more clinical significance if we had performed a larger number of cyclic mechanical tests. Fourth, we did not analyze the formation of a 3-mm gap between the tendon ends, as is common in biomechanical studies of tendon repair. However, the primary objective of our technique was not to maintain the tendon ends together but rather to allow the repair of the canine calcaneal tendon during chronic ruptures, in which the torn tendon ends are retracted and cannot be physiologically re-appositioned. The UHMWPE implant, therefore, serves as a synthetic tendon augmentation and allows the reinsertion of the canine calcaneal tendon directly into the calcaneus (Buttin *et al*., 2020a). Different kinds of sutures and suturing techniques now need to be investigated in order to find a method to increase the mechanical strength of the PTF, which was found to be the weakest fixation modality in our study.

Altogether, the present findings and previously published data show that the mechanical strength of proximal and distal fixations of the UHMWPE implant should be sufficient for calcaneal tendon repair in dogs from a biomechanical and *ex-vivo* point of view. If this type of canine calcaneal tendon repair ruptures, it will be at the level of the PTF.

Acknowledgments

We thank Mrs Cooke-Martageix E. and Mr Cooke R. for copyediting, and Dupeyroux J., Ph.D. for his support in the statistical analysis.

Author contributions

Buttin P., DVM, implanted the anatomic samples, Goin B., Ph.D. Student, processed the data, wrote the article, and revised the manuscript, Crumière A. J. J., Ph.D., wrote the article and revised the manuscript, Viguier E., DVM, Ph.D., ECVS, Massenzio M., Ph.D., Lafon Y., Ph.D., and Cachon T., DVM, Ph.D., ECVS, developed the experimental protocol and revised the manuscript.

Conflict of interest

The authors have no conflicts of interest to declare.

Funding

The present study was funded by Novetech Surgery but carried out independently by the University of Lyon, VetAgro Sup.

References

Ambrosius, L., Arnoldy, C., Waller, K.R., III, Little, J.P. and Bleedorn, J.A. 2015. Reconstruction of chronic triceps tendon avulsion using synthetic mesh graft in a dog. Vet. Comp. Orthop. Traumatol. 28, 220–224.

Aoki, A., Imade, S. and Uchio, Y. 2019. Effect of the positional relationship between the interference screw and the tendon graft in the bone tunnel in ligament reconstruction. J. Orthop. Surg. 27, 1–9.

Baltzer, W.I. and Rist, P. 2009. Achilles tendon repair in dogs using the semitendinosus muscle: surgical technique and short-term outcome in five dogs. Vet. Surg. 38, 770–779.

Blanc, Q., Goin, B., Rafael, P., Moissonnier, P., Carozzo, C., Buttin, P., Cachon, T. and Viguier, E. 2019. Effect of the number of interference screws for the fixation of an intra-articular cranial cruciate ligament prosthesis in dogs: Biomechanical study. Comput. Methods Biomech. Biomed. Engin. 22, S102–S104.

Buttin, P., Goin, B., Cachon, T. and Viguier, E. 2020a. Repair of tendon disruption using a novel synthetic fiber implant in dogs and cats: the surgical procedure and three case reports. Vet. Med. Int. 2020, 4146790.

Buttin, P., Goin, B., Giraud, N., Viguier, E. and Cachon, T. 2020b. Biomechanical analysis of an original repair of an achilles tendon rupture in dogs: preliminary results. Comput. Methods Biomech. Biomed. Engin. 23, S52–S54.

Cocca, C.J., Duffy, D.J., Kersh, M.E. and Moore, G.E. 2020. Influence of interlocking horizontal mattress epitendinous suture placement on tendinous biomechanical properties in a canine common calcaneal laceration model. Vet. Comp. Orthop. Traumatol. 33, 205–211.

Corr, S.A., Draffan, D., Kulendra, E., Carmichael, S. and Brodbelt, D. 2010. Retrospective study of Achilles mechanism disruption in 45 dogs. Vet. Rec. 167, 407–411.

Duffy, D.J., Chang, Y.-J., Fisher, M.B. and Moore, G.E. 2020a. Effect of partial vs complete circumferential epitendinous suture placement on the biomechanical properties and gap formation of canine cadaveric tendons. Vet. Surg. 49, 1571–1579.

Duffy, D.J., Chang, Y.-J., Gaffney, L.S., Fisher, M.B. and Moore, G.E. 2019. Effect of bite depth of an epitendinous suture on the biomechanical strength of repaired canine flexor tendons. Am. J. Vet. Res. 80, 1043–1049.

Duffy, D.J., Curcillo, C.P., Chang, Y.-J., Gaffney, L., Fisher, M.B. and Moore, G.E. 2020b. Biomechanical evaluation of an autologous flexor digitorum lateralis graft to augment the surgical repair of gastrocnemius tendon laceration in a canine *ex vivo* model. Vet. Surg. 49, 1545–1554.

Dunlap, A.E., Kim, S.E. and McNicholas, T.W.,Jr. 2016. Biomechanical evaluation of a non-locking pre-manufactured loop suture technique compared to a three-loop pulley suture in a canine calcaneus tendon avulsion model. Vet. Comp. Orthop. Traumatol. 29, 131–135.

Frame, K., Ben-Amotz, O., Simpler, R., Zuckerman, J. and Ben-Amotz, R. 2019. The use of bidirectional barbed suture in the treatment of a complete common calcanean tendon rupture in a dog: long-term clinical and ultrasonographic evaluation. Clin. Case Rep. 7, 1565–1572.

Gall, T.T., Santoni, B.G., Egger, E.L., Puttlitz, C.M. and Rooney, M.B. 2009. *In vitro* biomechanical comparison of polypropylene mesh, modified three-loop pulley suture pattern, and a combination for repair of distal Canine Achilles' Tendon Injuries. Vet. Surg. 38, 845–851.

Goin, B., Buttin, P., Cachon, T. and Viguier, E. 2020. Biomechanical comparison of two suturing techniques during Achilles tendinoplasty in dogs: preliminary results. Comput. Methods Biomech. Biomed. Engin. 23, S128–S129.

Goin, B., Rafael, P., Blanc, Q., Cachon, T., Buttin, P., Carozzo, C., Chabrand, P. and Viguier, E. 2019. Biomechanical analysis of a ligament fixation system for CCL reconstruction in a canine cadaver model. Comput. Methods Biomech. Biomed. Engin. 22, S109–S111.

Hirpara, K.M., Sullivan, P.J. and O'Sullivan, M.E. 2008. The effects of freezing on the tensile properties of repaired porcine flexor tendon. J. Hand Surg. Am. 33, 353–358.

Jopp, I. and Reese, S. 2009. Morphological and biomechanical studies on the common calcaneal tendon in dogs. Vet. Comp. Orthop. Traumatol. 22, 119–124.

Kása, F., Kása, G. and Prieur, W.D. 1994. Traumata von sehnen und sehnenscheiden. In praktikum der undeklinik. Eds., Niemand, H.G. and P.F. Suter. Berlin, Hamburg: Parey Verlag, pp: 198–199.

Katayama, M. 2016. Augmented repair of an achilles tendon rupture using the flexor digitorum lateralis tendon in a toy poodle. Vet. Surg. 45, 1083–1086.

Kessler, I. 1973. The "grasping" technique for tendon repair. Hand. 5, 253–255.

Meeson, R.L., Davidson, C. and Arthurs, G.I. 2011. Soft-tissue injuries associated with cast application for distal limb orthopaedic conditions. A retrospective study of sixty dogs and cats. Vet. Comp. Orthop. Traumatol. 24, 126–131.

Moores, A.P., Comerford, E.J., Tarlton, J.F. and Owen, M.R. 2004a. Biomechanical and clinical evaluation of a modified 3-loop pulley suture pattern for reattachment of canine tendons to bone. Vet. Surg. 33, 391–397.

Moores, A.P., Owen, M.R. and Tarlton, J.F. 2004b. The three-loop pulley suture versus two locking-loop sutures for the repair of canine achilles tendons. Vet. Surg. 33, 131–137.

Morton, M.A., Thomson, D.G., Rayward, R.M., Jiménez-Peláez, M. and Whitelock, R.G. 2015a. Repair of chronic rupture of the insertion of the gastrocnemius tendon in the dog using a polyethylene terephthalate implant. Early clinical experience and outcome. Vet. Comp. Orthop. Traumatol. 28, 282–287.

Morton, M.A., Whitelock, R.G. and Innes, J.F. 2015b. Mechanical testing of a synthetic canine gastrocnemius tendon implant. Vet. Surg. 44, 596–602.

Nielsen, C. and Pluhar, G.E. 2006. Outcome following surgical repair of achilles tendon rupture and comparison between postoperative tibiotarsal immobilization methods in dogs: 28 cases (1997–2004). Vet. Comp. Orthop. Traumatol. 19, 246–249.

O'Broin, E.S., Earley, M.J., Smyth, H. and Hooper, A.C.B. 1995. Absorbable sutures in tendon repair: a comparison of PDS with prolene in rabbit tendon repair. J. Hand Surg. Br. 20, 505–508.

Purchase, R., Mason, R., Hsu, V., Rogers, K., Gaughan, J.P. and Torg, J. 2007. Fourteen-year prospective results of a high-density polyethylene prosthetic anterior cruciate ligament reconstruction. J. Long Term Eff. Med. Implants 17, 13–19.

Schulz, K.S., Ash, K.J. and Cook, J.L. 2019. Clinical outcomes after common calcanean tendon rupture repair in dogs with a loop-suture tenorrhaphy technique and autogenous leukoreduced platelet-rich plasma. Vet. Surg. 48, 1262–1270.

Wilson, L., Banks, T.A., Luckman, P. and Smith, B. 2014. Biomechanical evaluation of double krackow sutures versus the three-loop pulley suture in a canine gastrocnemius tendon avulsion model. Aust. Vet. J. 92, 427–432.

Zellner, E.M., Hale, M.J. and Kraus, K.H. 2018. Application of tendon plating to manage failed calcaneal tendon repairs in a dog. Vet. Surg. 47, 439–444.

Zhang, A.L., Lewicky, Y.M., Oka, R., Mahar, A. and Pedowitz, R. 2007. Biomechanical analysis of femoral tunnel pull-out angles for anterior cruciate ligament reconstruction with bioabsorbable and metal interference screws. Am. J. Sports Med. 35, 637–642.